

Preparation of Chitosan Bicomponent Nanofibers Filled with Hydroxyapatite Nanoparticles via Electrospinning

Kai Shen, Qiaoling Hu, Liang Chen, Jiacong Shen

Department of Polymer Science and Engineering, Key laboratory of Macromolecule Synthesis and Functionalization of Ministry of Education, Zhejiang University, Hangzhou 310027, People's Republic of China

Received 9 February 2007; accepted 28 November 2008

DOI 10.1002/app.29832

Published online 26 October 2009 in Wiley InterScience (www.interscience.wiley.com).

ABSTRACT: Chitosan (CS) bicomponent nanofibers with an average diameter controlled from 100 to 50 nm were successfully prepared by electrospinning of CS and poly(vinyl alcohol) (PVA) blend solution. Finer fibers and more efficient fiber formations were observed with increased PVA contents. On this contribution, a uniform and ultra-fine nanofibrous CS bicomponent mats filled with hydroxyapatite (HA) nanoparticles were successfully electrospun in a well devised condition. An increase in the contents of HA nanoparticles caused the conductivity of the blend solution to increase from 1.06 mS/cm (0 wt % HA) to 2.27 mS/cm (0.5 wt % HA), 2.35 mS/cm (1.0 wt % HA),

respectively, and the average diameter of the composite fibers to decrease from 59 ± 10 nm (0 wt % HA) to 49 ± 10 nm (0.5 wt % HA), 46 ± 10 nm (1.0 wt % HA), respectively. SEM images showed that some particles had filled in the nanofibers whereas the others had dispersed on the surface of fibers, and EDXA results indicated that both the nanoparticles filled in the nanofibers and those adhered to the fibers were HA particles. © 2009 Wiley Periodicals, Inc. *J Appl Polym Sci* 115: 2683–2690, 2010

Key words: electrospinning; chitosan; hydroxyapatite; nanofibers

INTRODUCTION

Electrospinning is a straightforward, convenient, and inexpensive method to fabricate polymer fibers with diameters in the range of microns down to nanometers.^{1,2} Nanofibers have interesting characteristics such as very large surface area-to-volume ratio and high porosity with very small pore size. Therefore, nanofibers can be the promising materials for many biomedical applications.^{3–5} Chitosan (CS) has been proven to be biologically renewable, biodegradable, no antigenic, biocompatible,⁶ and used in wound dressing, drug delivery system, and various tissue engineering applications.^{7–11} The CS scaffold for the bone tissue engineering has been widely investigated and shown to enhance formation of the bone tissue both *in vitro* and *in vivo*.^{12,13} Hydroxyapatite (HA) was used in various biomedical fields such as dental

material, bone substitute, and hard tissue paste. HA can accelerate the formation of bone-like apatite on the surface of scaffold due to its good osteoinductivity and osteoconductivity.¹⁴ Nanoscale inorganic particles, which have displayed unique physical and chemical properties, can be used in numerous physical, biological, biomedical, and pharmaceutical applications. HA nanoparticle has been widely used in many biomedical fields such as tissue engineering, drug delivery, artificial teeth, and bone cement, because of its good properties such as biocompatibility, osteoconductivity, bioactivity, and low solubility.^{15–18} Recently, a few attempts have been made to prepare CS-based nanofibers by electrospinning for bone tissue engineering, with various degrees of success. By using trifluoroacetic acid/dichloromethane solvent, Yamamoto and coworkers¹⁹ fabricated CS/poly(vinyl alcohol) (PVA) nanofibers with the diameters from 220 to 650 nm. Zhang and coworkers²⁰ prepared CS/poly ethylene oxide (PEO) nanofibers for bone tissue engineering with mean diameter 115 ± 10 nm by adding dimethylsulphoxide (DMSO) as a cosolvent and studied the cellular compatibility of these nanofibers.

It is difficult to fabricate pure CS with high molecular weight in aqueous acetic acid, because the repulsive interaction among the polycations along the CS chains is thought to prevent sufficient chain entanglement, which is necessary for electrospinning.²¹ The existence of the PVA in this study is to improve the

Correspondence to: Q. Hu (huql@zju.edu.cn).

Contract grant sponsor: National Natural Science Foundation of China; contract grant numbers: 50173023, 50333020, 50773070.

Contract grant sponsor: Key Project of Foundation Research Project of China; contract grant number: 2005CB623902.

Contract grant sponsor: Key Science and Technology Special Project of Zhejiang province, China; contract grant number: 2008C11087.

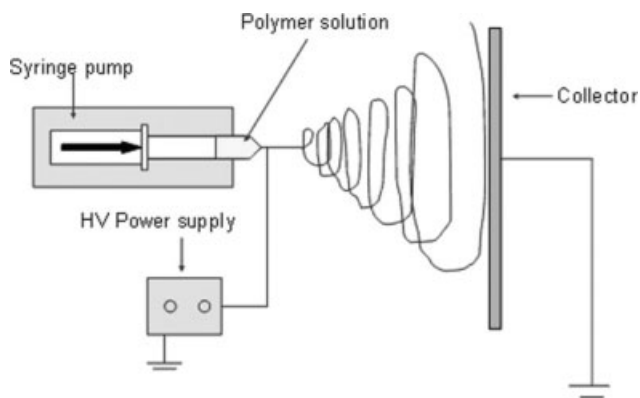


Figure 1 Schematic diagram of the electrospinning apparatus.

electrospinning process ability. As a water-soluble macromolecule, PVA possesses favorable electrospinning process ability as well as biocompatibility. In addition, it is reported that there were possible hydrogen bonds between CS and PVA molecules, which could weaken the strong interaction in CS itself and facilitate CS/PVA electrospinnability.²²

The aim of this work is to prepare ultrafine nanofibers by adjusting the CS/PVA volume ratio and

the parameters of electrospinning, without using organic solvent that usually has poor biocompatibility, and additionally to prepare novel bone scaffolds based on electrospun CS bicomponent nanofibers filled with HA nanoparticles.

EXPERIMENTAL

Materials

CS (91% deacetylated, $M_n = 56.3 \times 10^4$) was supplied by Qindao Haihui (People's Republic of China). PVA (88% hydrolyzed, average $M_w = 88000$) was purchased from ACROS Company (Belgium). HA nanoparticles were supplied by Nanjing Haitai Nanomaterials (People's Republic of China).

Electrospinning

PVA was dissolved in deionized water at a concentration of 9 wt % and CS was dissolved in 90% concentrated acetic acid at 2.5 wt %. The PVA solution was mixed with CS solution in the specified volume ratios and then electrospun at the following parameters (tip-target distance = 10–25 cm, flow rate = 0.3–1.5 mL/h, Voltage = 10–40 kV). To investigate the

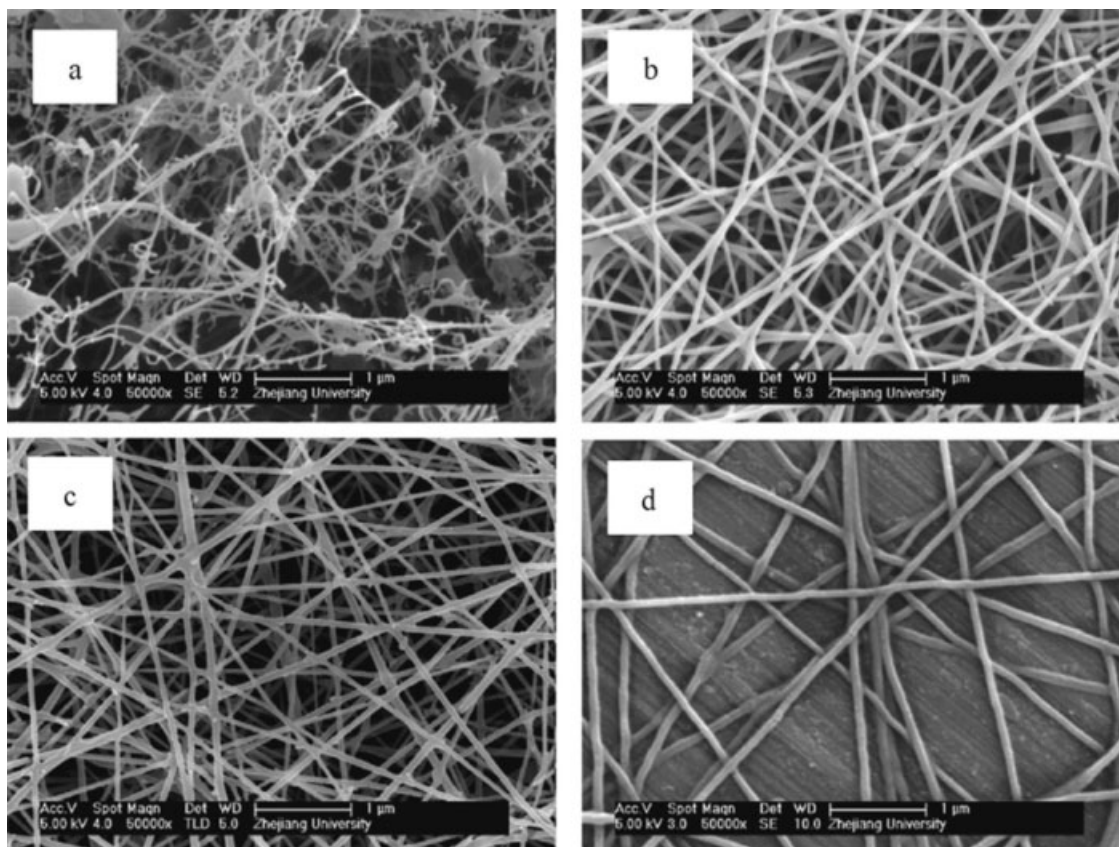


Figure 2 SEM images of the CS and PVA blended nanofibers electrospun under different volume ratios of CS/PVA. (a) 90/10, (b) 80/20, (c) 70/30, (d) 50/50. Electrospinning parameters: Voltage = 40 kV, flow rate = 0.5 mL/h, tip-target distance = 10 cm. Magnification: panel (a–d, $\times 50$ k).

effect of filler contents, either 0.5 or 1.0% (w/v) of HA nanoparticles were mixed in CS/PVA (50/50, v/v) blend solution.

During electrospinning, a high voltage power was applied to the polymer solution placed in a syringe with an alligator clip attaching to the syringe needle. The applied DC voltage was adjusted at 10–40 kV. The solution was delivered to the blunt needle (0.58 mm) tip with a syringe pump (WZ-500C2, Zhejiang, China) to control the solution flow rate. Fibers were collected on an electrically grounded aluminum foil, which was horizontally placed 10–20 cm away from the needle tip. In the electrospinning process, we have tried to find the optimum parameters for the electrospinning, such as applied voltage, flow rate, tip-collector distance, and so on. So the typical distance between the syringe tip and the collector was not a fixed value, but at 10–25 cm. Figure 1 shows the schematic diagram of the electrospinning apparatus.

Measurements

The viscosity of polymer solution was measured by a Brookfield digital viscometer (Model DV-E) at 20°C. The conductivity of polymer solution was measured

by a conductivity meter (DDS-11A, Shanghai, People's Republic of China) at 25°C. The morphology of electrospun fibers was observed by field emission scanning electron microscopy (FE-SEM, FEI-SIRION) (JAPAN HITACHI S-570). A small piece of the aluminum foil on which the electrospun fibers were collected was adhered to the sample base, and then a gold coating was applied on the sample to make sure the surface of it electrically conductive. The gold coating was uniform and about 100 nm thick. The average diameter of electrospun nanofibers was determined by measuring the diameters of the nanofibers at 60 different points in a 645×484 SEM image with the Image Pro software (IPP5.0.1). The diameters were presented as the average \pm standard deviation. Elemental analysis was carried out by an energy dispersive X-ray analyzer (EDXA) (OXFORD INCA energy dispersive x-ray detector), which was directly connected to FE-SEM, the environment mode and the sample preparing method were the same as those of SEM analysis. The accelerating voltage was 5.00 kV and the spot was 4.0. The content of HA in the final electrospun nanofibers was measured by the plasma inductance coupling mass spectrometry (Thermo Fisher Scientific X Series II).

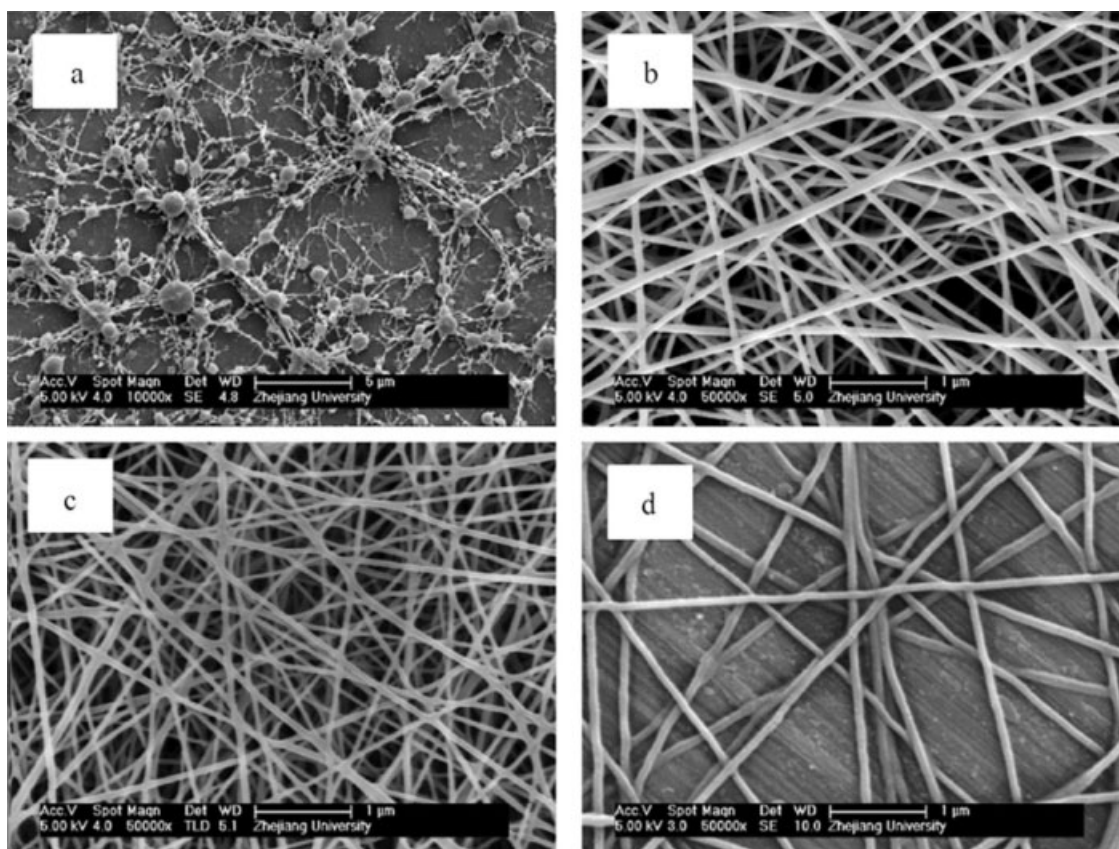


Figure 3 SEM images of the CS and PVA blended nanofibers electrospun under different applied voltage. (a) 10 kV, (b) 20 kV, (c) 25 kV, (d) 40 kV. Electrospinning parameters: 2.5% CS:9% PVA (v/v) = 50 : 50, flow rate = 0.5 mL/h, tip-target distance = 10 cm. Magnification: panel (a, $\times 10$ k), panel (b–d, $\times 50$ k).

RESULTS AND DISCUSSION

Electrospun CS/PVA mats

Figure 2 shows SEM images of the CS/PVA mats. When a small portion of the PVA was mixed with CS, as presented in Figure 2(a) (2.5% CS:9% PVA (v/v) = 90/10), the electrospun sample contained large-size beads and the fibers were fragile, incontinuous, and rough. As the content of the PVA solution increased (2.5% CS:9% PVA (v/v) = 80/20, 70/30), finer and more consistent nanofibers with an average diameter of 57 ± 10 nm, 60 ± 13 nm could be electrospun, but the diameters of nanofibers were not homogenous [Fig. 2(b,c)]. When equal volumes of the CS and PVA solutions were blended, ultrafine and uniform nanofibers with an average diameter of 90 ± 11 nm were obtained [Fig. 2(d)]. These results showed that the addition of PVA facilitated electrospinning CS into nanofibers, but the volume ratio of CS/PVA solutions should be less than 80/20. Li and Hsieh reported a similar tendency in the electrospinning of CS/PVA mats.²¹

In electrospinning process, when the electric field surpasses a threshold value where the electrostatic repulsion force of surface charges overcomes surface

tension, the charged fluid jet is ejected from the tip of the Taylor cone which refers to the cone observed in electrospray and hydrodynamic spray processes from which a jet of charged particles emanates above a threshold voltage. Thus, just like molecular weight, viscosity, conductivity and surface tension, voltage is also an important parameter in the electrospinning process.^{23,24}

The effect of the applied voltage on the morphological appearances and the sizes of the spun fibers was investigated. The mixed solution (2.5% CS : 9% PVA (v/v) = 50 : 50) was electrospun under an applied voltage of 10 kV, 20 kV, 25 kV, and 40 kV, respectively (tip-target distance = 10 cm, flow rate = 0.5 mL/h). At the applied voltage of 10 kV, large-size beads and fragile fibers were formed [Fig. 3(a)]. When the applied voltage was no less than 20 kV, which was high enough to overcome the surface tension of CS/PVA blend solution, smooth and homogenous bicomponent nanofibers were obtained [Fig. 3(b,c,d)]. The average diameters of the obtained bicomponent nanofibers were 56 ± 13 nm (20 kV), 59 ± 10 nm (25 kV), 90 ± 11 nm (40 kV), respectively. These results indicated an increase in the fiber diameter with increased applied voltage. Sheng and

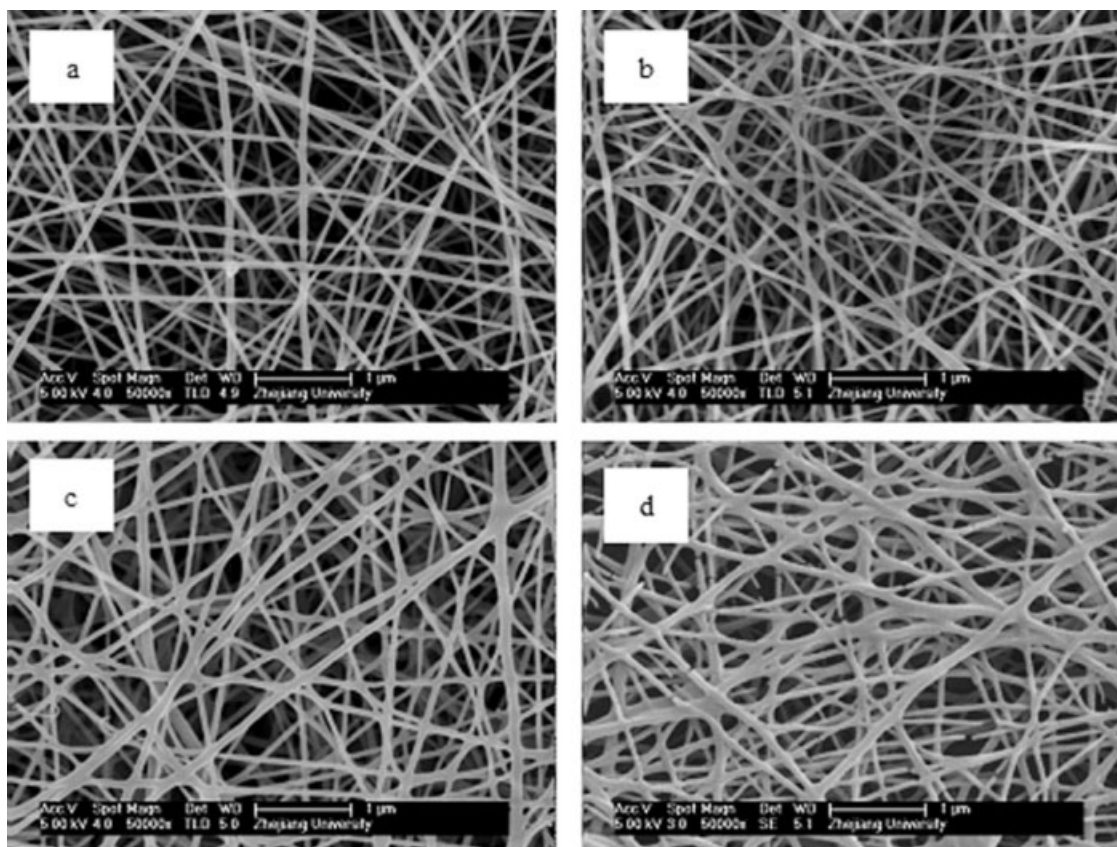


Figure 4 SEM images of the CS and PVA blended nanofibers electrospun under different flow rate. (a) 0.3 mL/h, (b) 0.5 mL/h, (c) 1.0 mL/h, (d) 1.5 mL/h. Electrospinning parameters: 2.5% CS:9% PVA (v/v) = 50 : 50, Voltage = 25 kV, tip-target distance = 10 cm. Magnification: panel (a–d), $\times 50$ k).

coworkers²⁵ reported a similar tendency in the electrospinning of PVA mats that there was a slightly increase in average fiber diameter with increasing applied electric field. Because of the increase in the electrostatic force acting on the charged jet, the solution would be removed from the tip more quickly as jet was ejected from Taylor cone, which reduced the tendency for the charged jet to be thinned down by both the coulomb repulsion force and the forces occurring during the bending instability.

As another important parameter in the process of electrospinning, the effect of the flow rate on the morphological appearances and the sizes of the spun fibers was also investigated. When the flow rate was at a low level, the tip of the Taylor cone was inclined to be blocked and the spinning speed would be too slow. Once the transmission rate of solution surpassed the rate of ejection caused by the electrostatic repulsive force, large-size beads and fragile fibers would be formed due to the continuous but unstable fluid jet. Figure 4 showed SEM images of nanofibers electrospun under different flow rate with the range from 0.3 mL/h to 1.5 mL/h (2.5% CS:9% PVA (v/v) = 50 : 50, applied voltage = 25 kV, tip-target distance =

10 cm). At the flow rate of 0.3 mL/h, smooth and homogenous bicomponent nanofibers with the average diameter of 54 ± 11 nm were obtained [Fig. 4(a)]. And at the flow rate of 0.5 mL/h, no distinct differences were observed [Fig. 4(b)]. But when the flow rate increased to 1.0 mL/h, inhomogeneous nanofibers with wider distribution were obtained, even though the average diameter didn't have much difference [Fig. 4(c)]. When the flow rate continued to increase to 1.5 mL/h, there was a phenomenon that the nanofibers became discontinuous and more inhomogeneous, some of which even ruptured [Fig. 4(d)]. So the flow rate should be controlled at 0.5 mL/h or so.

In the electrospinning process, the change of the tip-target distance under the same voltage will lead to the differences of the magnitude of, and time when the electrostatic repulsive force acted on the droplets of the blend solution, as well as the differences of evaporation time of the solvent. Therefore, the tip-target distance is a negligible parameter in the electrospinning process. Figure 5 showed the SEM images of the nanofibers electrospun under the following conditions (2.5% CS:9% PVA (v/v) = 50 : 50, applied voltage = 25 kV, flow rate = 0.5 mL/h) while the tip-

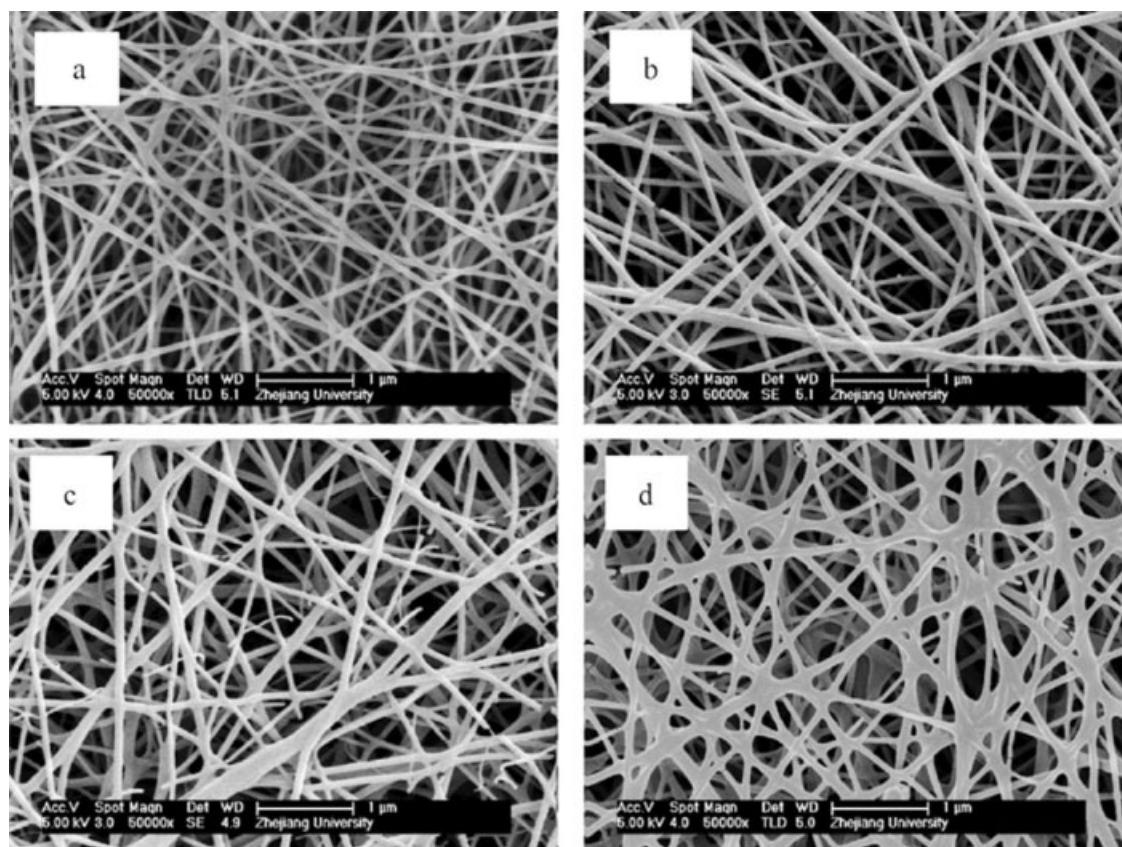


Figure 5 SEM images of the CS and PVA blend nanofibers electrospun under different tip-target distance. (a) 10 cm, (b) 15 cm, (c) 20 cm, (d) 25 cm. Electrospinning parameters: 2.5% CS:9% PVA (v/v) = 50 : 50, flow rate = 0.5 mL/h, Voltage = 25 kV. Magnification: panel (a–d, $\times 50$ k).

target distance ranging from 10 to 25 cm. When the tip-target distance was 10 cm or 15 cm, smooth and homogenous bicomponent nanofibers with the average diameter of 59 ± 10 nm and 56 ± 8 nm were obtained, respectively [Fig. 5(a,b)]. When the tip-target distance increased to 20 cm, the diameters of the nanofibers had a wider dispersion with the average diameter being 57 ± 18 nm, as well as the bifurcation and breakage of the incontinuous fibers could be observed [Fig. 5(c)]. When the tip-target distance was 25 cm, the obtained nanofibers had ribbon structures with poor morphology and bonded each other [Fig. 5(d)]. So the ideal tip-target distance should be in the range from 10 to 15 cm.

Electrospinning of CS/PVA blend solution with HA nanoparticles

The purpose of the HA used in this study is to improve osteoblast proliferation and differentiation on CS bicomponent mats. In the above study, smooth and uniform nanofibers with an average diameter of 59 ± 10 nm were obtained from the mixed solution (2.5%wtCS/9wt%PVA = 50/50) under the specified electrospinning parameters (Applied voltage = 25 kV,

tip-target distance = 10 cm, flow rate = 0.5 mL/h). Thus, various amounts of HA nanoparticles were mixed with the blend solution and then electrospun at the specified parameters. Figure 6(a) is the SEM image of HA nanoparticles, from which we can observe that in the blend solution, some nanoparticles dispersed well, whereas the other nanoparticles aggregated to form HA stack. SEM images [Fig. 6(b,c,d)] showed that ultrafine and uniform CS/PVA fibers filled with varied contents of HA were successfully fabricated. The average diameter of CS/PVA fibers was 59 ± 10 nm. When the content of HA increased from 0.5 wt % to 1 wt %, the average diameter of electrospun fibers was decreased from 49 ± 10 nm to 46 ± 10 nm. As shown in Table I, the increase of HA content led to an increase in the conductivity of blend solution from 1.06 mS/cm (0 wt % HA) to 2.27 mS/cm (0.5 wt % HA), 2.35 mS/cm (1.0 wt % HA), respectively. Therefore, the higher net charge density increased the electrical force exerted on the jet and decreased fiber diameter. It was reported that the addition of salts increases the charge density in the ejected jets, and thus, stronger elongation forces are imposed on them, due to the self-repulsion of the excess charges under the electrical field,

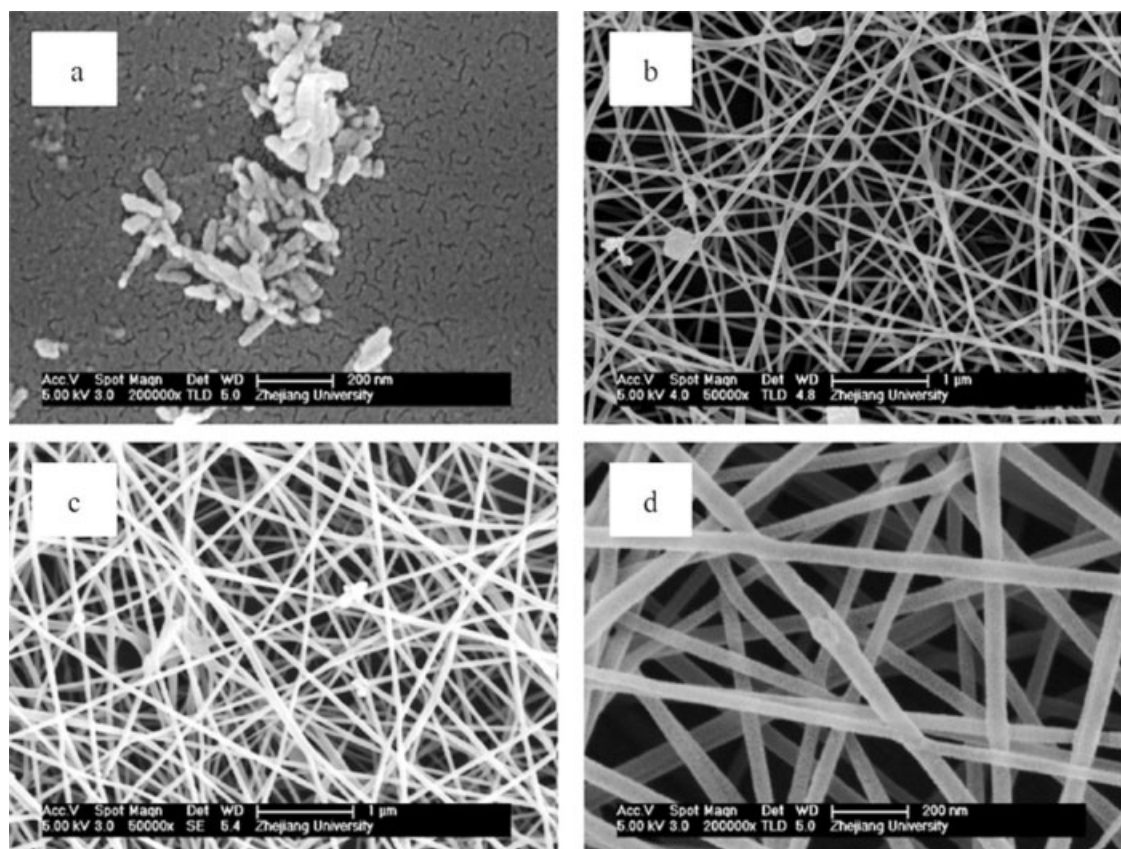


Figure 6 SEM images of (a) HA nanoparticles in the blend solution, electrospun nanofibers from (b) 2.5 wt % CS/9 wt % PVA = 50/50, HA 1 wt %; (c,d) 2.5 wt % CS/9 wt % PVA = 50/50, HA 0.5 wt %. Electrospinning parameters: tip-target distance = 10 cm, flow rate = 0.5 mL/h, Voltage = 25 kV. Magnification: panel (a,d, $\times 20$ k); panel (b,c, $\times 5$ k).

TABLE I
Physical Property of Mixed Solutions

Sample	CS (wt %)	PVA (wt %)	Ratio (v/v)	HA (wt %)	Viscosity (cp)	Conductivity (mS/cm)
1	2.5	9	50/50	0	486.2	1.06
2	2.5	9	50/50	0.5	613.5	2.27
3	2.5	9	50/50	1	596.2	2.35

resulting in the electrospun fibers having a substantially straighter shape and smaller diameter.²⁶ And similar phenomenon was reported by Youk and coworkers²⁷ in the preparation of PVA nanofibers containing silver nanoparticles and by Naebe et al.²⁸ in the preparation of PVA electrospun nanofibers with MWNT fillers. In addition, from the SEM images (Fig. 6), it was observed that some nanoparticles were filled in the nanofibers [Fig. 6(d)], whereas some aggregated particles ranged from 100 nm to less than 1 μm were

adhered to the surface of bicomponent nanofibers [Fig. 6(b,c)]. In the electrospinning process, the well-dispersed nanoparticles whose sizes were about 60–100 nm in length and 20–40 nm in width could be embedded in the fibers with the diameter about 50 nm. However, the aggregated particles whose sizes were more than 200 nm in length and 100 nm in width could not be embedded in the ultrafine fibers due to their large size, which led to some particles adhering to the nanofibers. It is preferable for the nanoparticles

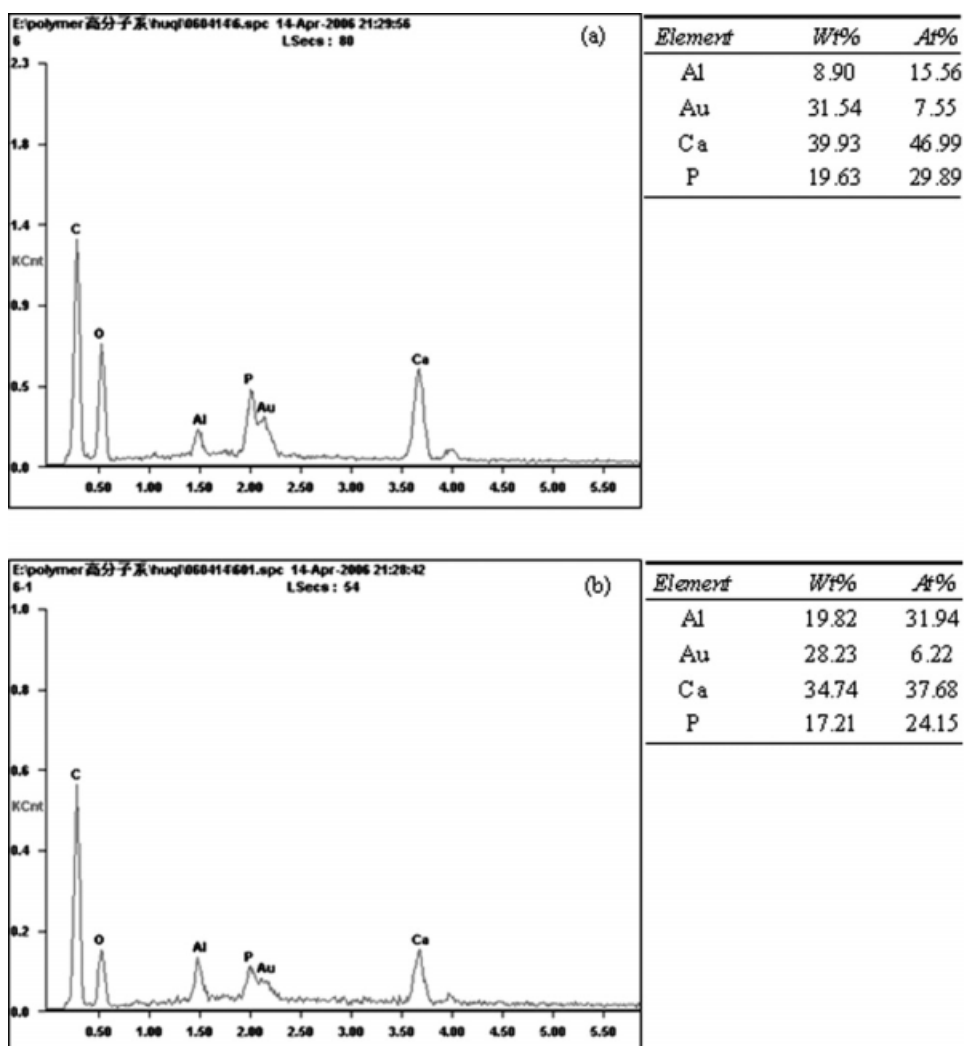


Figure 7 EDXA spectra of (a) nanoparticles filled in the CS bicomponent nanofibers (b) nanoparticles adhered to nanofibers.

to fill in the nanofibers. Once the nanoparticles disperse more equably and don't get aggregated, there will be more nanoparticles in the better location.

The EDXA spectra which was illustrated in Figure 7 showed that the Ca/P atom ratios of the nanoparticles filled in fibers and the aggregated particles adhered to fibers were 1.57 and 1.56, whereas those of HA were 1.67. Considering the error of the EDXA and the purity of HA, although there was slight difference between the Ca/P atom ratios of the nanoparticles and those of HA, it was confirmed that both the nanoparticles filled in fibers and particles adhered to the fibers were HA. Though the content of HA in the blend solution was only 0.5 wt % or 1.0 wt %, which seemed relatively low, the actual content of HA in the final electrospun nanofibers was not low, ~ 10% and 15%, respectively, according to the plasma inductance coupling mass-spectrometry. The increase of HA content was due to the evaporation of the solvent during the electrospinning process. This tendency could be observed from the EDXA spectra too. Because both HA and CS have favorable biocompatibility and bioactivity,²⁹ it is reasonably to conclude that the CS bicomponent mats possessed favorable biocompatibility and bioactivity.

CONCLUSIONS

A uniform and ultrafine nanofibrous CS bicomponent mats filled with HA nanoparticles was successfully electrospun in the following optimum condition: 2.5 wt % CS/9 wt % PVA = 50/50 blend solution, 0.5 wt % HA, applied voltage = 25 kV, tip-target distance = 10 cm, flow rate = 0.5 mL/h.

Some HA nanoparticles were filled in the fibers, whereas some particles were dispersed on the surface of fibers. The average diameter of the bicomponent fibers is 49 ± 10 nm. Because of the addition of HA in the electrospinning process without introducing organic solvent with poor biocompatibility, the mats are biocompatible and endowed with favorable osteoinductivity and osteoconductivity, which make them potentially useful in bone tissue engineering field.

References

1. Reneker, D. H.; Chun, I. *Nanotechnology* 1996, 7, 216.
2. Shin, Y. M.; Hohman, M. M.; Brenner, M. P.; Rutledge, G. C. *Appl Phys Lett* 2001, 78, 1149.
3. Kenawy, E. R.; Bowlin, G. L.; Mansfield, K.; Layman, J.; Simpson, D. G.; Sanders, E. H.; Wnek, G. E. *J Control Release* 2002, 81, 57.
4. Yoshimoto, H.; Shin, Y. M.; Terai, H.; Vacanti, J. P. *Biomaterials* 2003, 24, 2077.
5. Li, W. J.; Tuli, R.; Okafor, C.; Derfoul, A.; Danielson, K. G.; Hall, D. J.; Tuan, R. S. *Biomaterials* 2005, 26, 599.
6. Kumar, M. N. V. R. *React Funct Polym* 2000, 46, 1.
7. Hirano, S.; Itakura, C.; Seino, H.; Akiyama, Y.; Nonaka, I.; Kanbara, N. et al. *J Agric Food Chem* 1990, 38, 1214.
8. Aiedeh, K.; Gianasi, E.; Orienti, I.; Zecchi, V. *J Microencapsul* 1997, 14, 567.
9. Berger, J.; Reist, M.; Mayer, J. M.; Felt, O.; Gurny, R. *Eur J Pharm Biopharm* 2004, 57, 35.
10. Yagi, K.; Michibayashi, N.; Kurikawa, N.; Nakashima, Y.; Mizoguchi, T.; Harada, A. et al. *Biol Pharm Bull* 1997, 20, 1290.
11. Zhang, Y.; Zhang, M. Q. *J Biomed Mater Res* 2002, 62, 378.
12. Klokkevold, P. R.; Vandermark, L.; Kenney, E. B.; Bernard, G. W. *J Periodontol* 1996, 67, 1170.
13. Gutowska, A.; Jeong, B.; Jasionowski, M. *Anat Rec* 2001, 263, 342.
14. Sabokbar, A.; Pandey, R.; Diaz, J.; Quinn, J.; Murray, D. W. *J Mater Sci: Mater Med* 2001, 12, 659.
15. Sarvestani, A.; Jabbari, E. *Biomacromolecules* 2006, 7, 1573.
16. Sugawara; Yamane. et al. *Macromol Rapid Commun* 2006, 27, 441.
17. Sung; Shin. et al. *Nanotechnology* 2007, 18, 6.
18. Zhang; Nichols. et al. *J Biomed Mater Res A* 2007, 82, 373.
19. Ohkawa, K.; Cha, D. I.; Kim, H.; Nishida, A.; Yamamoto, H. *Macromol Rapid Commun* 2004, 25, 1600.
20. Bhattarai, N.; Edmondson, D.; Veis, O.; Matsen, F. A.; Zhang, M. Q. *Biomaterials* 2005, 26, 6176.
21. Li, L.; Hsieh, Y. L. *Carbohydrate Res* 2006, 341, 374.
22. Li, Y.; Haas, T. W.; Elie, A. G.; Bowlin, G. L.; Simpson, D. G.; Wnek, G. E. *Chem Mater* 2003, 15, 1860.
23. Hohman, M. M.; Shin, M. *Phys Fluids* 2001, 13, 2201.
24. Huang, Z. M.; Zhang, Y. Z.; Kotaki, M.; Ramakrishna, S. *Compos Sci Technol* 2003, 63, 2223.
25. Zhang, C. X.; Yuan, X. Y.; Wu, L. L.; Han, Y.; Sheng, J. *Eur Polym J* 2005, 41, 423.
26. Son, W. K.; Youk, J. H.; Lee, T. S.; Park, W. H. *Polymer* 2004, 45, 2959.
27. Jin, W. J.; Jeon, H. J.; Kim, J. H.; Youk, J. H. *Synth Met* 2007, 157, 454.
28. Naebe, M.; Lin, T.; Tian, W.; Dai, L. M.; Wang, X. G. *Nanotechnology* 2007, 18, 22.
29. Kong, L. J.; Gao, Y.; Lu, G. Y.; Gong, Y. D.; Zhao, N. M.; Zhang, X. F. *Eur Polym J* 2006, 42, 3171.